

Received: 2020.09.14  
Accepted: 2020.12.27  
Available online: 2021.01.13  
Published: 2021.03.12

# Citrus Alkaline Extracts Inhibit Senescence of A549 Cells to Alleviate Pulmonary Fibrosis via the $\beta$ -Catenin/P53 Pathway

Authors' Contribution:  
Study Design A  
Data Collection B  
Statistical Analysis C  
Data Interpretation D  
Manuscript Preparation E  
Literature Search F  
Funds Collection G

**BDE 1 Di Han**  
**CE 1 Yong Xu**  
**BD 1 Wen-Pan Peng**  
**AD 1,2 Fanchao Feng**  
**BD 1 Zhichao Wang**  
**BD 1 Cheng Gu**  
**AG 1,2 Xianmei Zhou**

1 Department of Respiratory Medicine, Affiliated Hospital of Nanjing University of Chinese Medicine, Nanjing, Jiangsu, P.R, China  
2 Department of Respiratory Medicine, Jiangsu Province Hospital of Chinese Medicine, Nanjing, Jiangsu, P.R, China

\* Di Han and Yong Xu contributed equally to this work

**Corresponding Author:**

Xian Mei Zhou, e-mail: [zhouxianmeijs@aliyun.com](mailto:zhouxianmeijs@aliyun.com)

**Source of support:**

This work was supported by the National Natural Science Foundation of China (No. 81673936), Jiangsu Provinces Colleges and Universities (Integration of Chinese and Western Medicine), and Postgraduate Research & Practice Innovation Program of Jiangsu Province (No. KYCX20\_1550)

**Background:** Idiopathic pulmonary fibrosis (IPF) is a disease related to aging, which has become increasingly prevalent as the population has aged. However, there remains no effective treatment for the disease. Alveolar epithelial type II cell (AEC II) senescence plays an important role in the occurrence and development of IPF. Therefore, enhancing our understanding of aging AEC IIs might facilitate the development of a new therapeutic strategy for the prevention and treatment of IPF. The aim of this study was to investigate the effect of citrus alkaline extracts (CAE) on senescence in A549 cells and elucidate the mechanism by which CAE function.





**Material/Methods:** Adriamycin RD (ARD) induces the senescence of A549 cells. Relevant indicators were identified following administration of 3 concentrations of CAE (50  $\mu$ g/mL, 100  $\mu$ g/mL, and 200  $\mu$ g/mL) to A549 cells.

**Results:** CAE inhibited senescence in ARD-induced A549 cells. It inhibited p16, p21, p53, and a senescence-associated secretory phenotype, and reduced expression of the senescence-related positive cells of  $\beta$ -galactosidase. Further study revealed that activation of the  $\beta$ -catenin signaling pathway is closely associated with p53. CAE inhibited senescence in A549 cells via the  $\beta$ -catenin/p53 pathway. Further, inhibition of  $\beta$ -catenin was associated with reduced expression levels of p53 and p21, and the anti-aging effects of CAE were enhanced. When expression of p53 was inhibited, expression levels of  $\beta$ -catenin also tended to decrease.

**Conclusions:** In summary, our study showed that CAE can inhibit aging in A549 cells to alleviate pulmonary fibrosis, and thus limit the secretion of the extracellular matrix and collagen in lung fibroblasts.

**Keywords:** **beta Catenin • Cell Aging • Tumor Suppressor Protein p53**

**Full-text PDF:** <https://www.medscimonit.com/abstract/index/idArt/928547>

 4108  1  7  60



## Background

Idiopathic pulmonary fibrosis (IPF) is a gradual, irreversible, and serious disease of unknown origin, which occurs predominantly in elderly individuals [1]. Primary manifestations include fibrosis and honeycomb-like changes in the subpleural and basal regions of the lungs and deposition of collagen and extracellular matrix (ECM) around the pulmonary fibrosis foci [2]. Gradual loss of lung function and increased fatigability are associated with disease progression. Histopathological findings show patterns similar to interstitial pneumonia, which is characterized by patchy involvement of distal airways and lung parenchyma, with areas of alveolar damage and fibrotic remodeling [3]. With the increase of the elderly population in the past 10 years, the incidence rate of IPF has increased correspondingly [4]. Epidemiological and clinical data indicate that IPF is a disease related to aging and is prevalent in elderly individuals. Further, the incidence and mortality rates of IPF increase with age [5].

The main pathogenesis of pulmonary fibrosis involves the damage of type II alveolar epithelial cells (AEC IIs), which releases a large number of inflammatory factors that activate lung fibroblasts and induces the secretion of large quantities of ECM [6,7], eventually leading to lung scarring and remodeling. Studies have shown that aging is a key factor that affects the initiation and development of IPF, in which AEC IIs senescence is closely related to the occurrence and development of pulmonary fibrosis [8]. Mechanisms involved in IPF disease development and progression include repetitive injury to the lung epithelium, activation and proliferation of myofibroblasts, and altered production of ECM, together resulting in the destruction of lung architecture and function [9,10]. Epidemiological investigations have demonstrated that IPF mainly occurs in individuals over 60 years of age. Indeed, accumulating evidence suggests that the induction of cellular senescence may play an important role in the pathogenesis of radiation-induced pulmonary fibrosis and other fibrotic lung diseases, including IPF and pulmonary fibrosis induced by bleomycin [11]. Senescent AEC IIs have been detected in fibrotic foci in the lungs of patients with IPF. Similarly, mice treated with bleomycin or thoracic irradiation demonstrate increases in senescent AEC IIs, the putative alveolar stem cells (ASCs) [12]. When AEC IIs/ASCs become senescent, they cannot self-renew and generate AEC to maintain the homeostasis of the alveolar epithelium and repair the epithelium after tissue injury; however, they continue to occupy the stem cell niche. In addition, senescent AEC II can set in motion a self-perpetuating vicious cycle of an abnormal tissue repair process and secondary senescence by initiating oxidative stress and inflammation. This in turn leads to the disruption of normal tissue structure and function, in part via reactive oxygen species and the senescence-associated

secretory phenotype (SASP), which eventually leads to pulmonary fibrosis [13].

Cellular senescence is regulated by complex signal transduction pathways, of which, the p53/p21 axis is one of the most critical [14]. As the central link, p53 controls senescence, and acetylated p53, with a longer half-life, enhances the capacity of p21 to promote transcription [15]. One study found increased expression levels of p53, p21, and p16 and activity of senescence-associated  $\beta$ -galactosidase (SA- $\beta$ -gal) in human IPF cells compared to in normal epithelial cells [16]. Wnt/ $\beta$ -catenin signaling is very important to the regulation of cell cycle progression among adult mammals [17] and is related to cell senescence, as indicated in previous studies [18]. These studies revealed that  $\beta$ -catenin activity in the AEC IIs of aged mice was significantly higher than that of young mice. Moreover, activated Wnt/ $\beta$ -catenin signaling accelerates hematopoietic stem cell failure [19], and fibroblast [20], thymocyte [21], and endothelial cell [22] aging and dysfunction.

As the largest fruit crop in the world, citrus has played an important role in human history [23]. China is one of the main birthplaces of citrus, and since ancient times, citrus plants have been an important source of traditional Chinese medicine [24]. The dry pericarp of Rutaceae has been used in traditional Chinese medicine and as a source of food [25]. It has been confirmed that active ingredients from the dry pericarp of citrus decrease blood lipid levels [26], and produce antitumor [27], antiinflammatory [28], antioxidative [29], and antifibrosis effects [30]. The material has been widely used in the treatment of hypertension, ulcerative colitis, pulmonary fibrosis, and other diseases. Previous studies have clarified the composition of CAE by high-performance liquid chromatography. This compound can reduce the occurrence of lung fibrosis in vivo and in vitro and inhibit fibroblast senescence by activating COX-2 [31,32].

A previous study reported that Wnt/ $\beta$ -catenin signaling-induced renal epithelial cell senescence is mediated via the p53/p21 pathway [33]. In systemic lupus erythematosus, Wnt/ $\beta$ -catenin signaling mediated bone marrow mesenchymal stem cell senescence via the p53/p21 pathway [34]. The  $\beta$ -catenin and p53 expression in patients' lung tissue with pulmonary fibrosis has been determined to be significantly elevated compared to that in patients not affected by the disease; however, whether AEC II senescence is induced by the  $\beta$ -catenin/p53 pathway remains unclear. Therefore, in this study, we aimed to determine whether CAE prevents the progression of pulmonary fibrosis by inhibiting senescence in A549 cells via the  $\beta$ -catenin/p53 pathway.

## Material and Methods

### Reagents and Antibodies

The dried citrus peel was purchased from the Jiangsu Provincial Hospital of Traditional Chinese Medicine (Nanjing, China). The CAE was then prepared as previously described. Dickkopf-1 (DKK1) was purchased from R&D Systems (USA); dimethyl sulfoxide, fetal bovine serum, Dulbecco's modified Eagle's medium and trypsin were purchased from Gibco, Thermo Fisher Scientific-CN (Shanghai, China); penicillin and streptomycin were purchased from Biological Industries (HaEmek, Israel); platelet-derived growth factor a (PDGF-a), PDGF-b, tumor necrosis factor  $\alpha$  (TNF- $\alpha$ ), matrix metalloproteinases-7 (MMP-7), CyclinD1, connective tissue growth factor (CTGF),  $\alpha$ -smooth muscle aorta ( $\alpha$ -SMA), collagen I, collagen III,  $\beta$ -catenin, glycogen synthase kinase-3 $\beta$  (GSK-3 $\beta$ ),  $\beta$ -actin,  $\beta$ -tubulin, and GAPDH were purchased from Proteintech (Wuhan, China); and p53, p21, and p16 were purchased from Abcam (Cambridge, UK).

### Cell Culture

A549 cells and MRC-5 human lung fibroblasts were obtained from the China Cell Type Culture and Collection Center (Wuhan, China) and were cultured in DMEM with 10% fetal bovine serum supplemented with 100 U/mL penicillin G and 100  $\mu$ g/mL streptomycin. The cells were maintained at 37°C in a humidified 5% CO<sub>2</sub> incubator. For experiments involving Adriamycin RD (ARD)-induced senescence, A549 cells were treated with ARD (0.01  $\mu$ M) for 48 h. Then, the medium containing the ARD was removed and cells were starved for 24 h. After the addition of fresh medium, the cells were used for aging SA- $\beta$ -gal-positive cells using the SA- $\beta$ -gal test.

### Cell Co-culture

The A549 cells were treated with ARD (0.01  $\mu$ M) for 48 h. Then, the medium containing ARD was removed and the cells were starved for 24 h with different concentrations of CAE (50  $\mu$ g/mL, 100  $\mu$ g/mL, 200  $\mu$ g/mL). Next, the supernatant containing CAE was removed, the cells were washed 3 times with phosphate-buffered saline (PBS), and fresh medium was added for 48 h. Next, the conditioned supernatant (without CAE) was transferred to the MRC-5 cells [35]. The supernatant was applied to the MRC-5 cells for 3 days, and the cells were then used for western blotting and enzyme-linked immunosorbent assay (ELISA).

### SA- $\beta$ -gal Staining

The activity of SA- $\beta$ -gal in cultured A549 cells was assayed using the senescence-associated  $\beta$ -galactosidase staining kit from Beyotime (Nanjing, China), according to the manufacturer's

instructions. The SA- $\beta$ -gal-positive cells were examined under an optical microscope and were analyzed via Image J software version 1.52e.

### Western Blotting

The cultured cells were observed to lyse in radioimmunoprecipitation assay buffer containing 1% phenylmethylsulfonyl fluoride from Beyotime (Nanjing, China), and total protein levels were quantified by the Pierce bicinchoninic acid protein analysis kit (Thermo Scientific; Rockford, IL, USA). Proteins (20 g/well) were segregated via sodium dodecyl sulfate-polyacrylamide gel electrophoresis, and were subsequently moved to a hydrophilic polyvinylidene fluoride membrane (Merck MILL; Darmstadt, Germany). Next, the membrane was incubated with 5% dried skimmed milk powder in tris-buffered saline with 0.1% Tween 20 at 25°C for 1 h. Then, the membrane and primary antibody were incubated overnight at 4°C. Proteins were detected by incubating with a rabbit or a mouse IgG (H&L) antibody labeled with a peroxidase enzyme (Plano, TX, USA). The visualization of target bands was accomplished using a super-enhanced luminol-based chemiluminescent western blot detection kit (Yeasen; Shanghai, China). Protein levels were then standardized using  $\beta$ -tubulin,  $\beta$ -actin, or GAPDH.

### The Isolation of RNA and Real-time Quantitative Polymerase Chain Reaction

Total RNA was obtained by using a Trizol reagent (Invitrogen; Carlsbad, CA, USA), according to the manufacturer's instructions. Using the 5 $\times$ All-in-One RT MasterMix (Applied Biological Materials Inc; Richmond, BC, Canada), cDNA was extracted via reverse transcription. Expression levels of mRNA were evaluated via quantitative real-time polymerase chain reaction (PCR) using EvaGreen 2 $\times$ qPCR Master Mix (ABMI). Relative expression levels of mRNA target genes were determined by normalizing values to the expression levels of GAPDH. The comparative  $\Delta\Delta$ CT method was used for data analysis. The synthetic primers were obtained from Sangon Biotech (SB, Shanghai, China). The primer sequence is shown in **Table 1**.

### Immunofluorescence Staining

The A549 cells were immobilized for 30 min with 4% paraformaldehyde, incubated for 20 min with 0.5% Triton X-100, and washed 3 times with PBS. Then, nonspecific binding sites were blocked by incubating for 30 min at 25°C with 10% goat serum, and frozen cells and sections were incubated at 4°C with the anti- $\beta$ -catenin (1: 50) and anti-p53 (1: 100) antibodies. Next, the cells were stirred for 1 h at 25°C with FITC-labeled (1: 4000; Immunoway Biotechnology, USA) and Alexa-Fluor 647 (1: 500, Beyotime) secondary antibodies and washed with PBS. The A549 cells were stained 3 times with

**Table 1.** Primer sequences qRT-PCR.

Gene	Forward primer	Reverse primer
GAPDH	GGTGTCTCCTCGCACTCA	TGGTCCAGGGTTTCTTACTCC
PDGF-a	TTCGCAGGAAGAGAAGTATTGAGGAAG	CCGTGAAGGCTGGCACTTGAC
PDGF-b	TCTGCTGCTACCTGCGTCTGG	CATCTTCATCTACGGAGTCTCTGTGC
MMP-7	CCACTCACCTGCTGCTACTCATT	CTGCTGCTGGTGATCCTCTTGAG
CTGF	AGCTGCCTACCGACTGGAAGAC	GGTGGTTCTGTGCGGTGTGC
TNF- $\alpha$	GCGACGTGGAACGGCAGAAG	GAATGAGAAGAGGCTGAGACATAGGC
CyclinD1	TGGATTGATTCGAAATCTTGCC	GAACAAGCAACTGAAGTAGTCG
GSK-3 $\beta$	AGGAGAACCAATGTTTCGTAT	ATCCCCTGGAATATTGGTTGT
Collagen I	CGGCCTGCTGAAACCTC	GGGAGCACCACTTCACCGG
Collagen III	CCTTCGACTTCTCCTCAGCC	TTCGTGCAACCATCCTCCA
$\alpha$ -SMA	CTTGGCTTGCTTGTCAGG	CGGACAGGAATTGAAGCGGA
$\beta$ -catenin	TGAGGACAAGCCACAAGATTAC	TCCACCAGAGTAAAAGAACG

4',6-diamidino-2-phenylindole (DAPI). The exposure of target genes was obtained via visualization using the fluorescence microscopy.

## ELISA

The collagen I and collagen III levels within the supernatant of cultured cells were evaluated using an ELISA kit (Shanghai Westtang Bio-Tech Co, China), according to the manufacturer's instructions. The results were based on 3 experiments.

## Statistics Analysis

All experiments were conducted at least 3 times, and the data were expressed as mean $\pm$ SD. GraphPad Prism software version 8.0 was used to visualize the analysis, and statistical significance was determined using the Tukey-corrected, one-way ANOVA. Values of  $P < 0.05$  were regarded as statistically significant.

## Results

### ARD Induced A549 Cell Senescence

ARD is an anticancer drug that can induce senescence in a variety of cell types. Senescent cells typically produce increased levels of SA- $\beta$ -gal activity and secrete proinflammatory cytokines, a phenomenon referred to as SASP. As we have shown in a previous study, A549 cells exhibit senescent behavior after ARD (0.01  $\mu$ M) had been added for 48 h [36]. Cellular hypertrophy was used as the cell senescence marker. By visualizing cellular morphology in the present study, we found that A549 cells treated with ARD (0.01  $\mu$ M) for 48 h were larger and more

numerous than untreated cells (Figure 1A). SA- $\beta$ -gal has been identified as a general marker of aging. We observed a significant increase in the number of SA- $\beta$ -gal-positive cells in the A549 cells 48 h after ARD treatment as compared with control-treated A549 cells (Figure 1A, 1B). Western blot analysis revealed that the SASP of A549 cells treated with ARD was significantly more pronounced than that of normal cells (Figure 1C, 1D), which indicated that ARD induced senescence in A549 cells.

### CAE Inhibited the Aging of A549 Cells Induced by ARD

In order to assess the effect of CAE on aging in A549 cells, we analyzed the SASP associated with pulmonary fibrosis. The factors we monitored included PDGF-a, TNF- $\alpha$ , PDGF-b, MMP-7, CyclinD1, and CTGF. The senescent cells can secrete multiple SASPs, including cytokines, chemokines, matrix remodeling proteases, and growth factors, which can promote proliferation and tissue deterioration [13]. CTGF is a key additional biomarker of aging and cellular senescence [37]. PDGF isoforms and PDGF receptors have important functions in the regulation of growth and survival of various cell types [38]. These wound-associated senescent cells then promote optimal wound healing by secreting PDGF-A, a SASP factor, which promotes myofibroblast differentiation. PDGF secreted by senescent cells is a growth factor that regulates cell growth and the division of pericytes, which cover endothelial cell channels to provide stability and control perfusion of blood vessels [39]. We found that the treatment with CAE effectively reduced the number of SA- $\beta$ -gal-positive cells in a dose-dependent manner (Figure 2A, 2B). Western blotting revealed that after 24 h of CAE treatment, the expression levels of PDGF-a, TNF- $\alpha$ , PDGF-b, CyclinD1, and CTGF in senescent A549 cells were significantly reduced. Protein expression levels of MMP-7 also tended to decrease, but the levels did not statistically differ from those

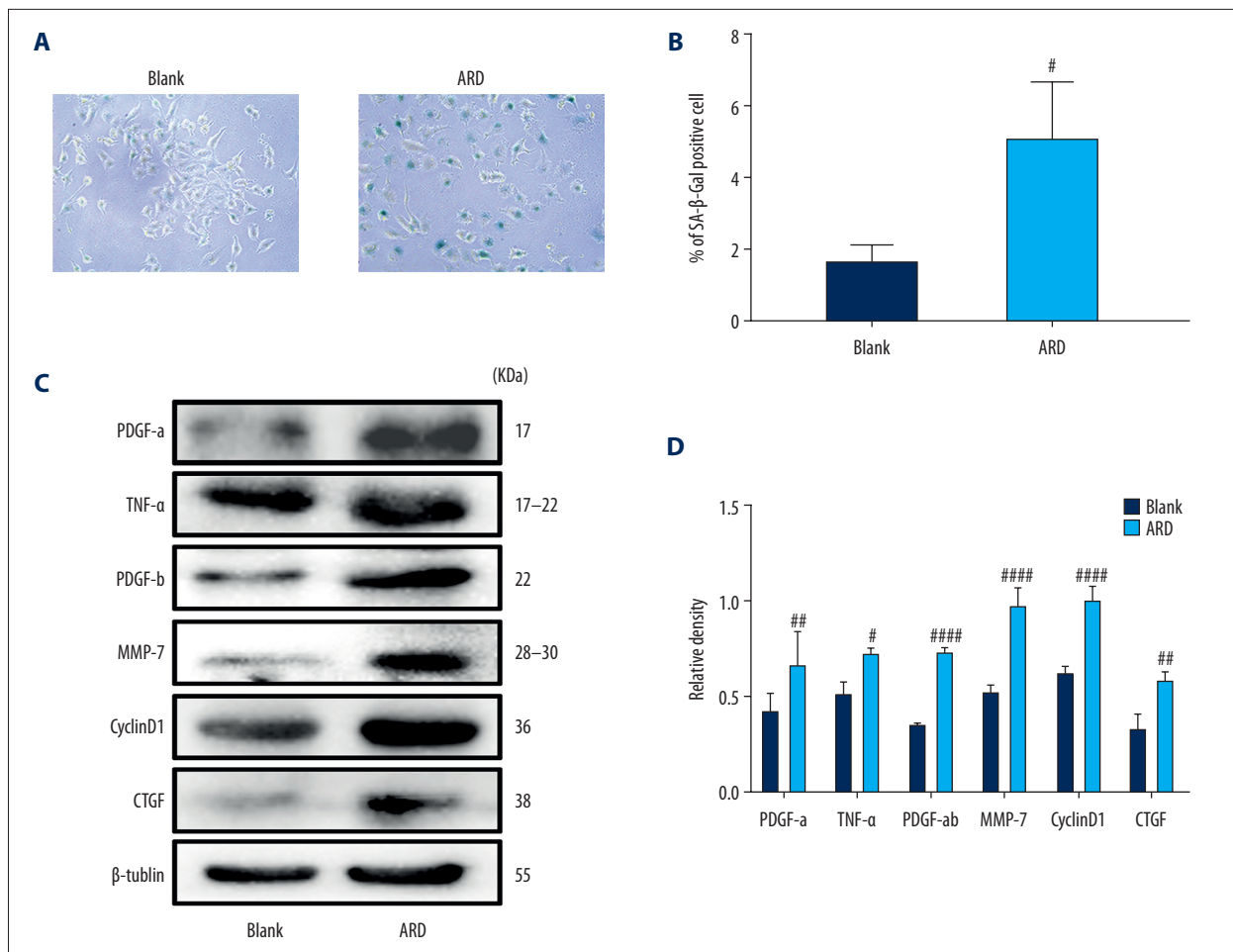


**Figure 1.** Adriamycin RD (ARD)-induced senescence in A549 cells. **(A, B)** The analysis of senescence-associated  $\beta$ -galactosidase staining (SA- $\beta$ -Gal). The SA- $\beta$ -Gal-positive cell percentages were scored; the mean $\pm$ SD of data from at least 3 separate experiments are visualized. Magnification:  $\times 200$  #  $P < 0.05$  vs Blank. **(C, D)** Western blot analysis of PDGF-a, TNF- $\alpha$ , PDGF-b, MMP-7, CyclinD1, and CTGF in A549 cells. Each group was assessed in triplicate, and experiments were repeated 3 times. Bar graphs show the relative quantification. #  $P < 0.05$ , ##  $P < 0.01$ , and ####  $P < 0.0001$  vs Blank.

of the control-treated cells (**Figure 2C**). However, mRNA levels of MMP-7 decreased in a dose-dependent manner after CAE treatment (**Figure 2D**). As a functional biomarker of aging, p16 plays an important role in cell senescence. After the treatment of CAE, the expression levels of p16 proteins decreased significantly, and levels of p16 mRNA displayed the same trend (**Figure 2E**). Our results indicated that CAE was capable of inhibiting aging in ARD-induced A549 cells.

### CAE Inhibited the Expression of P53 and $\beta$ -catenin in A549 Cells

Although previous results indicated that CAE inhibited senescence in A549 cells, the mechanism by which CAE functions remains unclear. To understand the preliminary mechanism by which CAE modulates senescence in A549 cells, we explored the activation state of key signals known to regulate the process of

senescence. When cells become senescent, DNA binding and the transcriptional activity of p53 increase, promoting target gene transcription [40]. This induces cell cycle arrest, mainly through p21 and other cell cycle-dependent kinase inhibitors. Western blotting revealed that after ARD-induced senescence, the protein expression levels of p53 and p21 increased, while CAE treatment inhibited expression of both proteins and their transcripts in a dose-dependent manner (**Figure 3A, 3B**). Previous studies have indicated that Wnt/ $\beta$ -catenin signaling is related to cell senescence and GSK-3 $\beta$  is its downstream target, which negatively regulates the exposure of  $\beta$ -catenin. The western blot results indicated that after ARD treatment, levels of  $\beta$ -catenin were significantly upregulated and expression levels of GSK-3 $\beta$  were downregulated. After 24 h of treatment with CAE, levels of  $\beta$ -catenin decreased, while GSK-3 $\beta$  levels gradually increased; the mRNA expression levels were consistent with these results (**Figure 3C, 3D**). Immunofluorescence



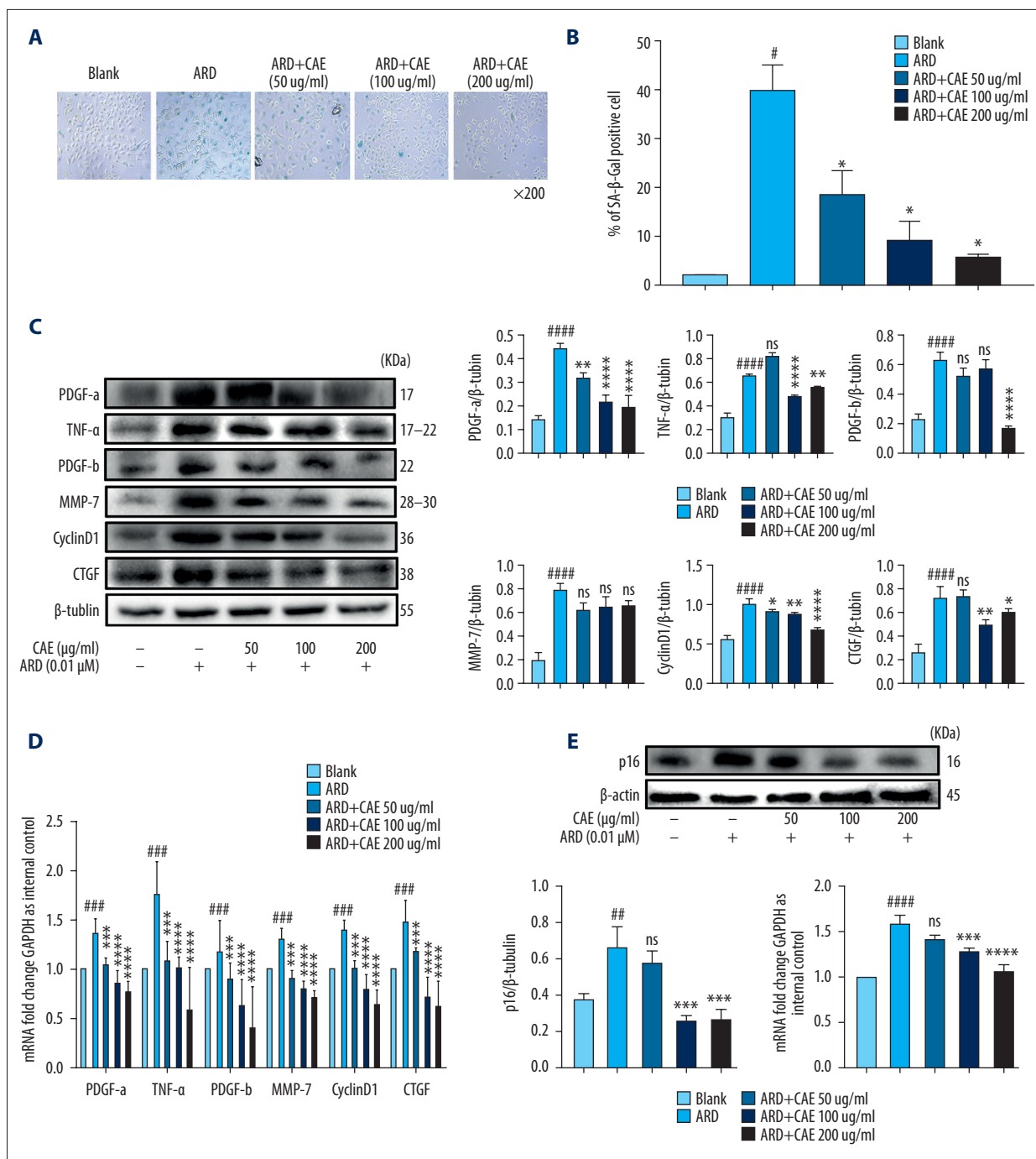


**Figure 2.** Citrus alkaline extracts (CAE) inhibited Adriamycin RD (ARD)-induced aging in A549 cells. **(A, B)** The analysis of senescence-associated β-galactosidase staining (SA-β-Gal). The SA-β-Gal-positive cells percentages were scored; the mean±SD of data from at least 3 separate experiments are visualized. #  $P<0.05$  vs Blank, \*  $P<0.05$  vs ARD. Magnification: ×200. **(C)** Western blot analysis of PDGF-a, TNF-α, PDGF-b, MMP-7, CyclinD1, and CTGF in A549 cells. Each group was operated in triplicate, and experiments were repeated 3 times. Bar graphs show the relative quantification. #  $P<0.05$ , ##  $P<0.01$ , ###  $P<0.001$ , and ####  $P<0.0001$  vs Blank; \*  $P<0.05$ , \*\*  $P<0.01$ , \*\*\*  $P<0.001$ , and \*\*\*\*  $P<0.0001$  vs ARD. **(D)** Real-time qPCR analysis of genes; relative expression of PDGF-a, TNF-α, PDGF-b, MMP-7, CyclinD1, and CTGF. #  $P<0.05$ , ##  $P<0.01$ , ###  $P<0.001$ , and ####  $P<0.0001$  vs Blank; \*  $P<0.05$ , \*\*  $P<0.01$ , \*\*\*  $P<0.001$ , and \*\*\*\*  $P<0.0001$  vs ARD. **(E)** The analysis of p16 in A549 cells by western blot. Each group was assessed in triplicate, and experiments were repeated 3 times. Bar graphs show the relative quantification, ##  $P<0.01$  vs Blank, \*\*  $P<0.01$ , and \*\*\*  $P<0.001$ . **(F)** Real-time qPCR analysis of genes and relative expression of p16. ###  $P<0.001$  vs Blank; \*\*  $P<0.01$ , \*\*\*  $P<0.001$ , and \*\*\*\*  $P<0.0001$  vs ARD.

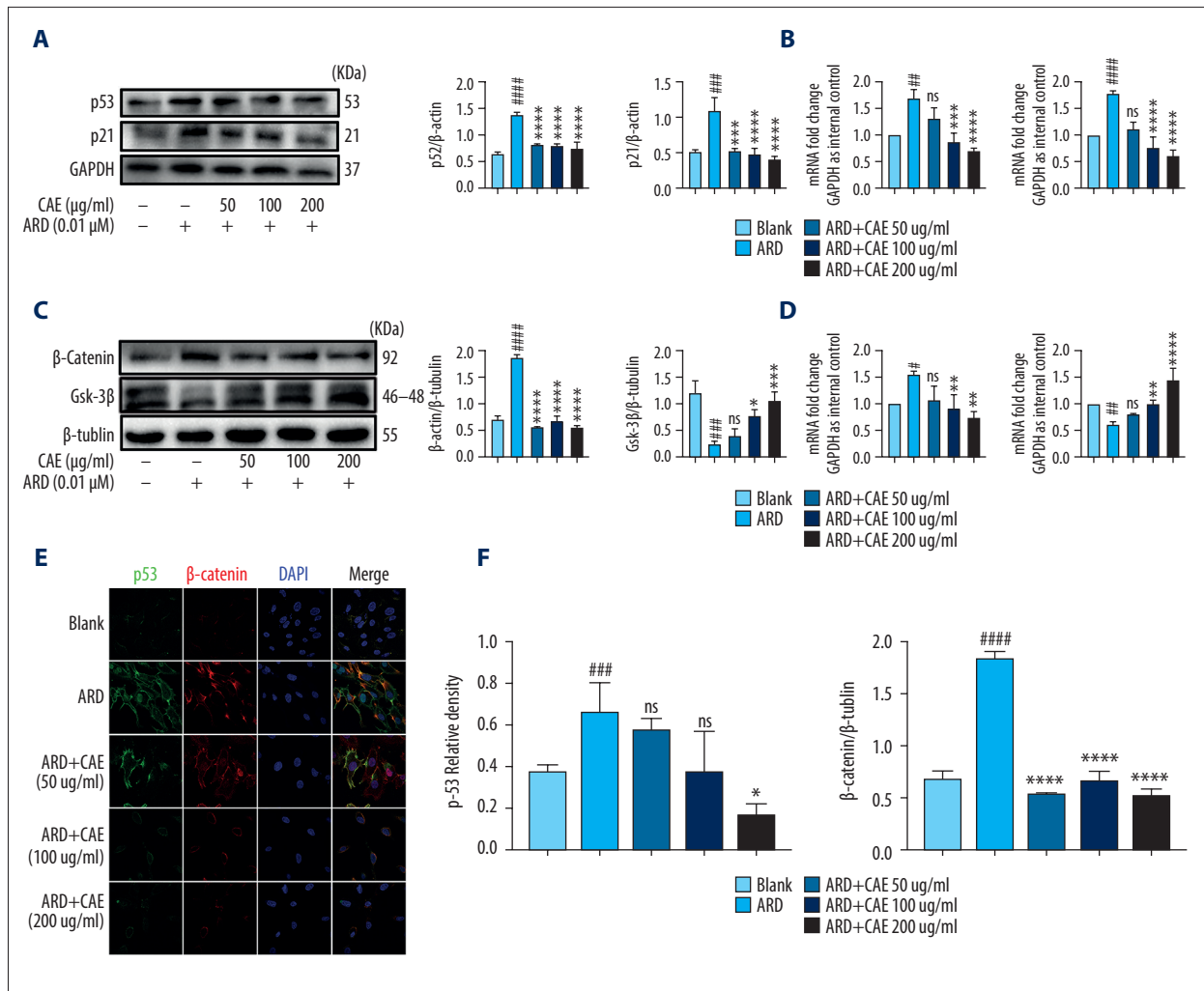


**Figure 3.** Citrus alkaline extracts (CAE) inhibited the expression of p53 and  $\beta$ -catenin in A549 cells. **(A)** The analysis of p53 and p21 in A549 cells by western blot. Each group was assessed in triplicate, and experiments were repeated 3 times. Bar graphs show the relative quantification. ###  $P < 0.001$ , ####  $P < 0.0001$  vs Blank; \*\*\*  $P < 0.001$ , \*\*\*\*  $P < 0.0001$  vs Adriamycin RD (ARD). **(B)** Real-time qPCR analysis of genes; relative expression of p53 and p21. ##  $P < 0.01$ , ####  $P < 0.0001$  vs Blank; \*  $P < 0.05$ , \*\*\*\*  $P < 0.0001$ , and ns=not significant vs ARD. **(C)** The analysis of  $\beta$ -catenin and GSK-3 $\beta$  in A549 cells by western blot. Each group was assessed in triplicate, and experiments were repeated 3 times. Bar graphs show the relative quantification, ##  $P < 0.01$  vs Blank, \*\*  $P < 0.01$ , \*\*\*  $P < 0.001$ , and ns=not significant vs ARD. **(D)** Real-time qPCR analysis of genes, relative expression of p16. ###  $P < 0.001$  vs Blank, \*  $P < 0.05$ , \*\*\*  $P < 0.001$ , and \*\*\*\*  $P < 0.0001$  vs ARD. **(E, F)** Immunofluorescence staining of p53 and  $\beta$ -catenin. DAPI was used to stain the nucleus. Scale bar, 50  $\mu$ m; ###  $P < 0.001$  vs Blank, \*  $P < 0.05$ , \*\*\*  $P < 0.001$ , and ns=not significant vs ARD.

assays revealed that the expression of p53 and  $\beta$ -catenin significantly increased 48 h after ARD treatment, but decreased 24 h after CAE treatment (**Figure 3E, 3F**). These findings indicate that CAE inhibited expression of p53, p21, and  $\beta$ -catenin in A549 cells, and CAE may inhibit senescence in A549 cells through the  $\beta$ -catenin/p53 pathway.

### CAE Inhibited A549 Senescence Through the $\beta$ -catenin/P53 Pathway

Previous studies have revealed a correlation between the p53 and Wnt signaling pathways. For example, downstream effector T-cell factor 4 (TCF-4) was identified as a transcriptional target of p53 [41]. Overexpression of  $\beta$ -catenin in the cytoplasm of human retinoblastoma cells enhanced the transcriptional activity of p53. Therefore, we used Wnt/ $\beta$ -catenin and p53 inhibitors to explore the relationship between the proteins. The results revealed that DKK1 and PTF- $\alpha$  did not induce cell

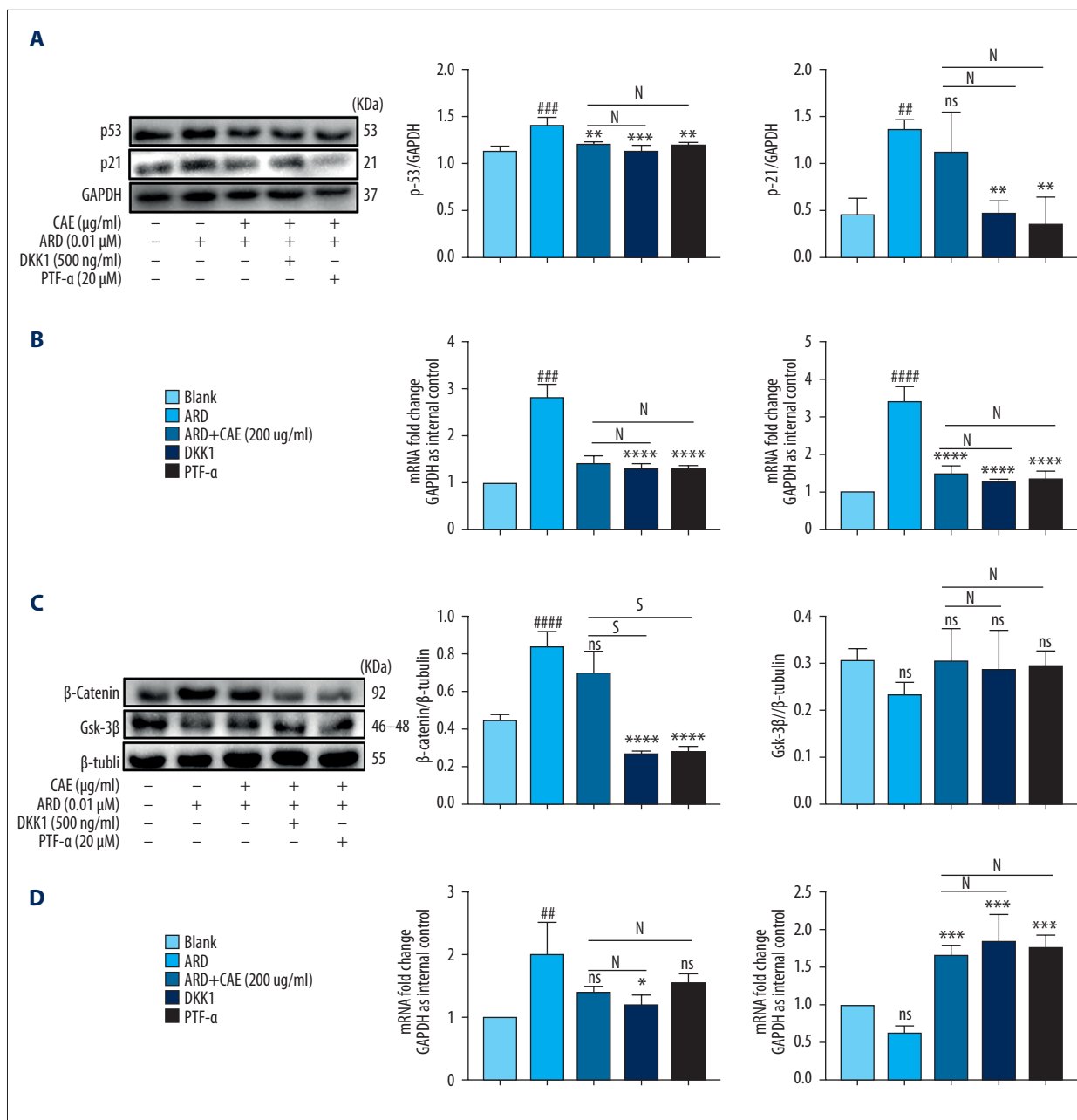


**Figure 4.** Citrus alkaline extracts (CAE) inhibited A549 senescence through the  $\beta$ -catenin/p53 pathway. **(A)** The analysis of p53 and p21 in A549 cells by western blot. Each group was assessed in triplicate, and experiments were repeated 3 times. Bar graphs show the relative quantification, ###  $P < 0.001$ , vs Blank, \*\*  $P < 0.01$ , \*\*\*  $P < 0.001$ , and ns = not significant vs Adriamycin RD (ARD); s,  $P < 0.05$ , N = not significant vs ARD+CAE. **(B)** Real-time qPCR analysis of genes; relative expression of p53 and p21. ####  $P < 0.0001$  vs Blank, \*\*\*\*  $P < 0.0001$  vs ARD; s,  $P < 0.05$ . N = not significant vs ARD+CAE. **(C)** Western blot analysis of  $\beta$ -catenin and GSK-3 $\beta$  in A549 cells. Each group was assessed in triplicate and experiments were repeated 3 times. Bar graphs indicate the relative quantification. ####  $P < 0.0001$  vs Blank, \*\*\*\*  $P < 0.0001$ , ns = not significant vs ARD; s,  $P < 0.05$ . N = no significant vs ARD+CAE. **(D)** The qPCR analysis of real-time genes relative, expression of p16. ##  $P < 0.01$  vs Blank, \*\*  $P < 0.05$ , \*\*\*\*  $P < 0.0001$ , and ns = not significant vs ARD; s,  $P < 0.05$ . N = no significant vs ARD+CAE.



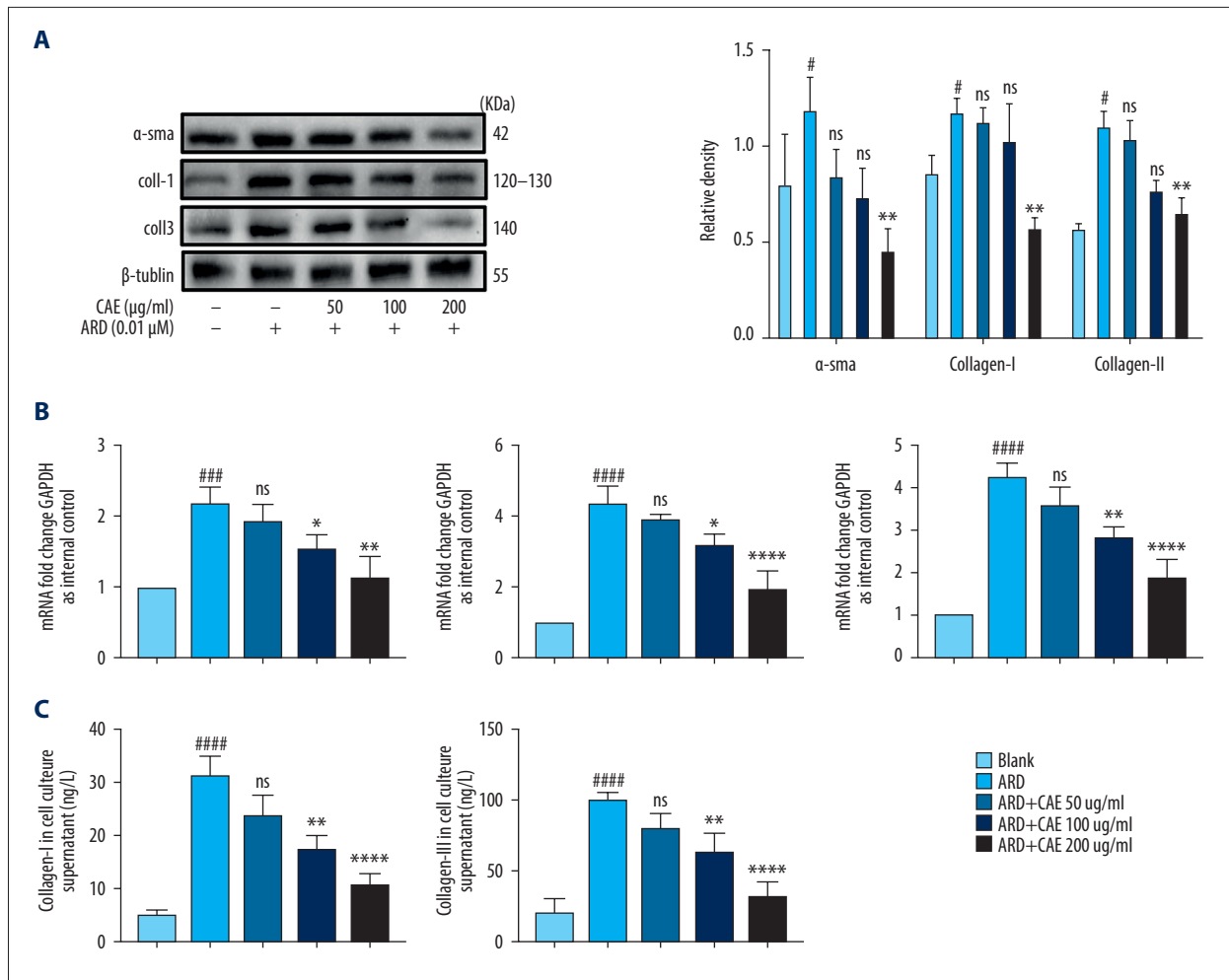


**Figure 5.** Citrus alkaline extracts (CAE) reduced expression levels of fibrosis markers in MRC-5 cells by inhibiting senescence in A549 cells. **(A)** An analysis of  $\alpha$ -SMA by western blot, collagen I, collagen III in MRC-5 cells. Each group was assessed in triplicate, and experiments were repeated 3 times. Bar graphs show the relative quantification, #  $P < 0.05$  vs Blank, \*\*  $P < 0.01$ , and ns=not significant vs Adriamycin RD (ARD). **(B)** Real-time qPCR analysis of genes, and relative expression of  $\alpha$ -SMA, collagen I, and collagen III. ###  $P < 0.001$ , ####  $P < 0.0001$  vs Blank, \*  $P < 0.05$ , \*\*  $P < 0.01$ , \*\*\*\*  $P < 0.0001$ , and ns=no significant vs ARD. **(C)** Determination of transforming collagen I and collagen III in the cell culture supernatant. The data are shown as mean $\pm$ SD. ####  $P < 0.0001$  vs Blank; ns=no significant \*\*  $P < 0.01$  and \*\*\*\*  $P < 0.0001$  vs ARD.

senescence (**Supplementary Figure 1**). After treating A549 cells with DKK1, the inhibitor of  $\beta$ -catenin, DKK1 inhibits of the WNT signaling pathway, and studies have shown that DKK1 changes WNT-induced epithelial cell proliferation in a dose-dependent manner in vitro [42]. In the present study,  $\beta$ -catenin protein expression was significantly downregulated, while p53 and expression levels of the downstream factor p21 also tended to decline. However, protein expression levels of GSK-3 $\beta$  increased, albeit non-significantly, and mRNA expression levels displayed the same trends (**Figure 4C, 4D**). Previous studies have shown that PFT- $\alpha$  has the ability to reversibly block p53-dependent transcriptional activation and apoptosis, as a specific inhibitor of the p53 signaling pathway. A 10- $\mu$ M concentration of PFT- $\alpha$  inhibited apoptotic death of C8 cells induced

by Dox, etoposide, Taxol, cytosine arabinoside, UV light, and gamma radiation [43]. In the present study, after treating A549 cells with PTF- $\alpha$ , the inhibitor of p53, levels of p53, p21, and  $\beta$ -catenin proteins significantly decreased, while the levels of GSK-3 $\beta$  expression increased. We observed that changes in the transcription levels of p53, p21,  $\beta$ -catenin, and GSK-3 $\beta$  corresponded to changes in protein levels (**Figure 4A, 4B**). It should be noted that the anti-aging effect of CAE can be enhanced by treating A549 cells with DKK1 and PTF- $\alpha$  and a high dose of CAE. As shown in **Figure 4**, in the senescent A549 cells pretreated with DKK1 and PTF, the effect of CAE on inhibiting the senescence of A549 cells seems to be enhanced. The protein expression of p21 and  $\beta$ -catenin was significantly increased compared with that of the CAE group (**Figure 4A, 4C**). Their

mRNA expression levels were consistent (Figure 4B, 4D). After inhibitor intervention, the protein expression of p53 showed a downward trend compared with that of the CAE group, and the mRNA expression of p53 and p21 showed the same trend, but there was no statistical significance (Figure 4B). Compared with the CAE group, after the intervention of inhibitors, the expression of GSK-3 $\beta$  showed an upward trend, and the expression of mRNA showed the same trend, but there was no statistical significance. These findings demonstrate that  $\beta$ -catenin and p53 interact, and CAE may inhibit senescence in A549 cells via the  $\beta$ -catenin/p53 pathway.

### CAE Reduced the Expression of Fibrosis Markers in MRC-5 Cells by Inhibiting the Senescence of A549 Cells

Studies have shown that some senescence-associated factors could induce senescence in normal cells, and senescence can be transferred to untransformed adjacent cells through the paracrine activity of SASP [44]. AEC II is a key factor that promotes the development of pulmonary fibrosis, and the pulmonary fibroblast is an important component needed for the development of pulmonary fibrosis. We observed that CAE could inhibit senescence in ARD-induced A549 cells and reduce the SASP. Next, we tested whether CAE had the capacity to regulate expression of fibrosis markers in MRC-5 cells by inhibiting senescence in A549 cells. We transferred the supernatant from A549 cells that were treated with ARD or CAE to cultures of MRC-5 cells, followed by a 3-day culture. Then, we detected the expression levels of lung fibrosis markers including  $\alpha$ -SMA, collagen I, and collagen III. Western blotting results revealed that the protein levels of  $\alpha$ -SMA, collagen I, and collagen III gradually decreased as CAE concentration increased. Further, mRNA levels corresponded to those determined for the proteins (Figure 5A, 5B). The presence of collagen I and collagen III in the supernatants of cultures was detected by ELISA. Results showed that the expression of collagen I and collagen III in the supernatant tended to decrease after CAE treatment relative to the levels associated with untreated cells (Figure 5C). Our results demonstrated that CAE inhibited the expression of  $\alpha$ -SMA, collagen I, and collagen III in lung fibroblasts by inhibiting senescence in A549 cells. Therefore, we believed that CAE may repress pulmonary fibrosis by inhibiting aging in AEC IIs.

## Discussion

Fibrosis is a common pathological feature of many lung diseases, including IPF, an aging-related disease of unknown etiology [4]. Our previous results suggested that CAE could effectively induce pulmonary fibroblast apoptosis of a normal and model mice, and its functioning mechanism was probably related to the p38/COX-2/Fas signaling pathway, regulated by oxidative stress [45]. Additionally, other previous findings illustrated that CAE regulates lung fibroblast senescence, which

is dependent on the COX-2/P53 pathway, suggesting that the inhibition of cellular senescence might represent an approach to control pro-fibrotic lung fibroblasts [32]. However, whether CAE can inhibit senescence in AEC IIs remains unclear, and the mechanism in IPF is unknown.

In IPF and an experimental pulmonary fibrosis model, AEC IIs showed obvious signs of aging [46]. AEC IIs are progenitor cells of the alveolar epithelium. In vitro, A549 cells are commonly used as a substitute for AEC IIs. ARD is an anticancer drug that can induce senescence in a variety of cell types. Our present study revealed that ARD-treated A549 cells experienced senescence and displayed SASPs, which affected lung fibroblasts in a paracrine manner.

Cell senescence is an evolutionary conservative state of stable replication stagnation that is induced by aging-associated stressors including telomere wear, oxidative stress, DNA damage, and proteomic instability [6]. These sources of stress are associated with the pathogenesis of IPF. Cellular senescence is now considered an important driving mechanism for chronic lung diseases, particularly IPF [47]. The aging of lung tissue ultimately results in structural remodeling of the ECM caused by alterations in the concentration and organization of ECM components such as collagen and elastin [48]. The tumor suppressor p53 induces cell cycle arrest, apoptosis, senescence, and innate immunity. This protein plays a central role in cell senescence, mainly by inducing the dephosphorylation of the cyclin-dependent kinase inhibitor p21 and by activating the cell cycle inhibitor retinoblastoma [49]. We also analyzed the p53/p21 pathway in the present study. Our results confirmed that the expression of the p53 and p21 proteins in A549 cells were significantly increased by ARD-induced senescence. Further, expression levels of p53 and p21 in A549 cells significantly decreased 24 h after CAE treatment.

Wnt signaling pathways are strictly regulated under physiological conditions. They play a key role in regulating cell fate and tissue regeneration [50]. Activation of the signaling of Wnt/ $\beta$ -catenin is accompanied by the accumulation of  $\beta$ -catenin in the cytoplasm,  $\beta$ -catenin's translocation into the nucleus, and its binding with T-cell factor/lymphocyte enhancer factor [41]. Wnt signaling can be divided into at least 3 different pathways, of which, the most extensively studied is the pathway of Wnt/ $\beta$ -catenin signaling. This classical signaling pathway is initiated by the extracellular ligand Wnt. Without the Wnt ligand, the  $\beta$ -catenin is phosphorylated via GSK-3 $\beta$  and subsequently degraded via the ubiquitin proteasome system [51]. As Wnt ligands connect to coiled receptors, the GSK-3 $\beta$  activity is then inhibited, non-phosphorylated  $\beta$ -Catenin levels are increased in the cytoplasm to then transfer to the nucleus to promote transcription of its various target genes [17]. Research by Chilosì et al [52] revealed that  $\beta$ -catenin plays a significant role in the development of fibrosis, and its aberrant activation

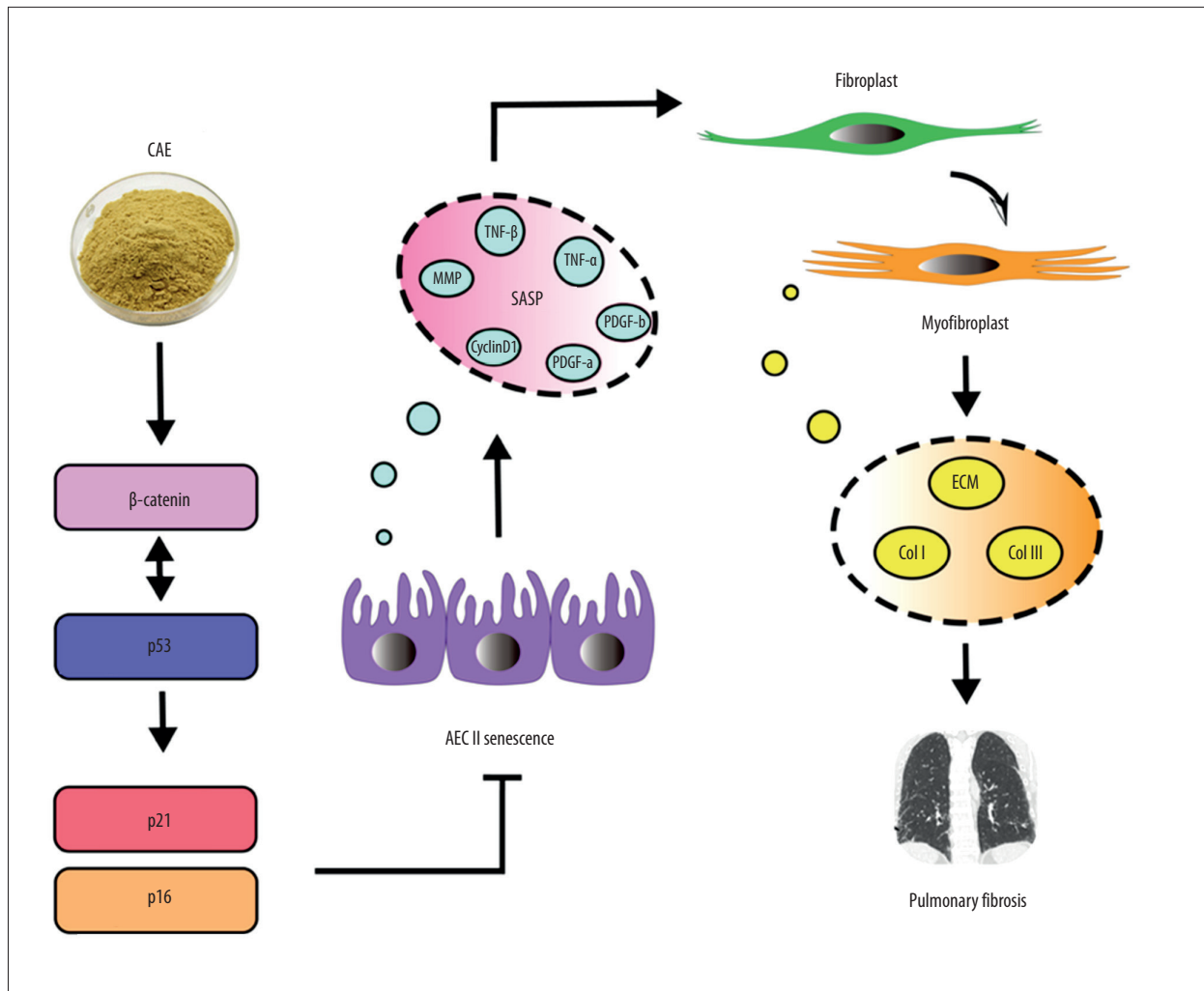


**Figure 6.** Citrus alkaline extract (CAE) inhibition, a proposed mechanism of alveolar epithelial type II cell (AEC II) senescence to alleviate pulmonary fibrosis via the β-Catenin/p53 pathway.

is a key feature of IPF. The signaling of Wnt/β-catenin controls the progenitor cells function and regulates tissue homeostasis in both developing and mature lungs. Previous studies have shown that the activation of Wnt/β-catenin has been observed in human and animal lungs, and is associated with pulmonary epithelial dysfunction [18]. In the present study, we have confirmed that increased β-catenin activity accelerates cell senescence. Our results also indicated that the signaling of Wnt/β-catenin modulates cell senescence. ARD showed the capacity to activate the signaling pathway of Wnt/β-catenin in A549 cells, which enhanced levels of β-catenin and reduced levels of GSK-3β. However, CAE treatment decreased expression levels of β-catenin and enhanced the expression of GSK-3β. This indicates that CAE may inhibit the Wnt/β-catenin pathway, which is related to cellular senescence.

Wnt/β-catenin signal transduction and the p53 pathway are key regulators of aging and are closely associated with heart

failure, systemic lupus erythematosus, kidney disease, cancer, and other diseases [53]. A feedback loop between β-catenin and p53 has been observed in colon cells. Any increase in β-catenin concentration in a cytoplasm leads to an activation of p53, which then promotes the proteasomal degradation of β-catenin [52]. Other studies have confirmed that the signaling of Wnt/β-catenin activation leads to p53 accumulation [54]. The signaling of Wnt/β-catenin regulates the proliferation and differentiation of the mesenchymal progenitor cells through the p53 pathway [55]. TCF-4 is a transcription factor with a key role in the signaling of Wnt/β-catenin. In cancer, p53 regulates the transcription of TCF-4, indicating a relationship between β-catenin and p53 [56]. One way in which p53 affects the Wnt signaling pathway involves DKK1. The DKK1 protein can inhibit Wnt activity, and is also transcriptionally upregulated by p53 [57]. Both p53 and β-catenin interact via an autoregulatory loop [58]. Elevated levels of β-catenin inhibit p53 degradation and thereby enhance p53 activity. This effect is

antagonized by active p53, which leads to the downregulation of protein levels of  $\beta$ -catenin [59]. It has been shown that the expression levels of Wnt/ $\beta$ -catenin and p53 in AEC IIs in patients with IPF are elevated as compared with those of individuals without IPF [60]. Our results indicated that  $\beta$ -catenin, p53, and p21 expression decreased after treatment with either DKK1 or PTF- $\alpha$ . This finding suggests that there is a link between the  $\beta$ -catenin pathway and the p53 pathway and that CAE can inhibit A549 senescence via the  $\beta$ -catenin/p53 pathway.

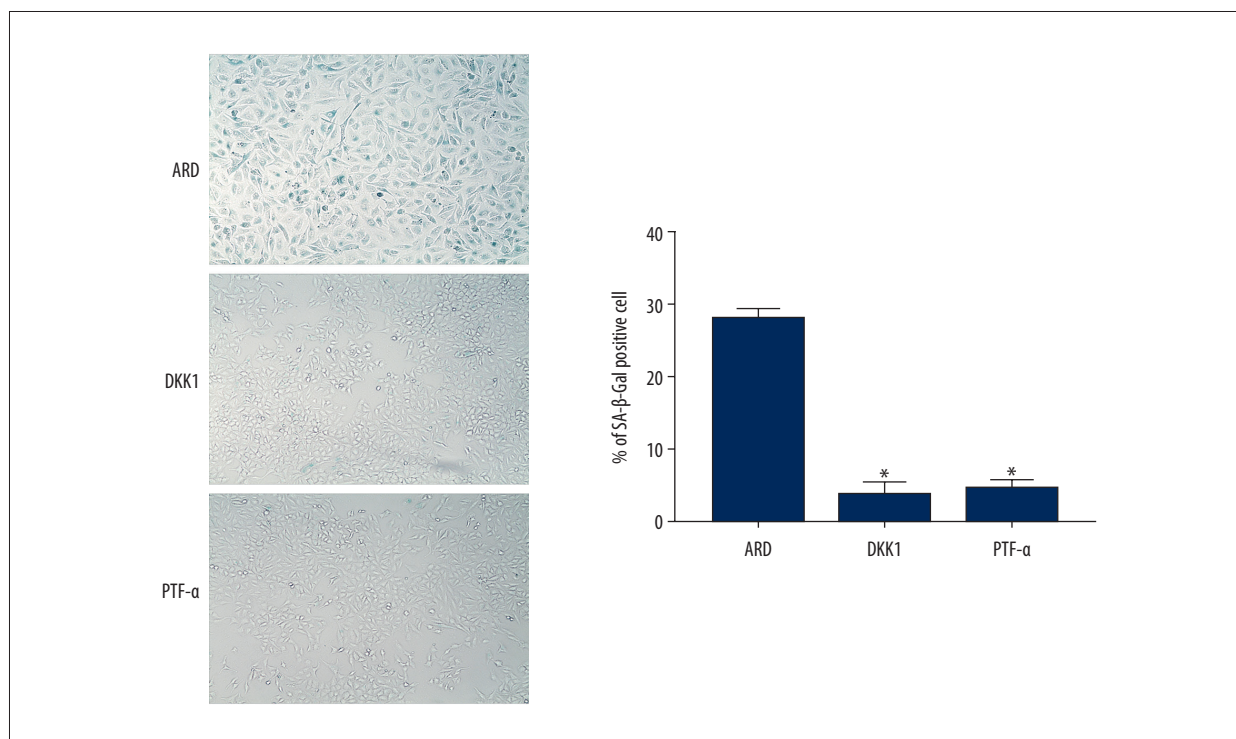
## Conclusions

We assessed the effect of CAE treatment on aging and elucidated the mechanism by which CAE inhibits senescence in A549 cells. Our results indicate that CAE inhibits senescence in A549 cells via the  $\beta$ -catenin/p53 pathway. The inhibition of epithelial senescence can alleviate pulmonary fibrosis. Therefore, our findings suggest that inhibiting epithelial cell senescence can limit pulmonary fibrosis (Figure 6). These findings indicate that CAE may be a promising therapeutic option for the treatment of IPF.

## Conflict of Interest

None.

## Supplementary Data



**Supplementary Figure 1.** DKK1 and PTF- $\alpha$  did not induce cell senescence. The analysis of senescence-associated  $\beta$ -galactosidase staining (SA- $\beta$ -Gal). The SA- $\beta$ -Gal-positive cells percentages were scored; the mean $\pm$ SD of data from at least 3 separate experiments are visualized. Magnification:  $\times 100$ , \*  $P < 0.05$  vs Adriamycin RD (ARD).



## References:

1. Tian Y, Li H, Qiu T, et al. Loss of PTEN induces lung fibrosis via alveolar epithelial cell senescence depending on NF- $\kappa$ B activation. *Aging Cell*, 2019;18:e12858
2. Upagupta C, Shimbori C, Alsilmi R, Kolb M. Matrix abnormalities in pulmonary fibrosis. *Eur Respir Rev*, 2018;27:180033
3. Moimas S, Salton F, Kosmider B, et al. miR-200 family members reduce senescence and restore idiopathic pulmonary fibrosis type II alveolar epithelial cell transdifferentiation. *ERJ Open Res*, 2019;5:00138-2019
4. Lederer DJ, Martinez FJ. Idiopathic pulmonary fibrosis. *N Engl J Med*, 2018;378:1811-23
5. Olson AL, Gifford AH, Inase N, et al. The epidemiology of idiopathic pulmonary fibrosis and interstitial lung diseases risk of a progressive-fibrosing phenotype. *Eur Respir Rev*, 2018;27:180077
6. Meiners S, Eickelberg O, Königshoff M. Hallmarks of the ageing lung. *Eur Respir J*, 2015;45:807-27
7. Wolters PJ, Collard HR, Jones KD. Pathogenesis of idiopathic pulmonary fibrosis. *Annu Rev Pathol*, 2014;9:157-79
8. Bagnato G, Harari S. Cellular interactions in the pathogenesis of interstitial lung diseases. *Eur Respir Rev*, 2015;24:102-14
9. Wolters PJ, Collard HR, Jones KD. Pathogenesis of idiopathic pulmonary fibrosis. *Annu Rev Pathol*, 2014;9:157-79
10. King TEJ, Pardo A, Selman M. Idiopathic pulmonary fibrosis. *Lancet*, 2011;378:1949-61
11. He Y, Thummuri D, Zheng G, et al. Cellular senescence and radiation-induced pulmonary fibrosis. *Transl Res*, 2019;209:14-21
12. Citrin DE, Shankavaram U, Horton JA, et al. Role of type II pneumocyte senescence in radiation-induced lung fibrosis. *J Natl Cancer Inst*, 2013;105:1474-84
13. Mailleux AA, Crestani B. Licence to kill senescent cells in idiopathic pulmonary fibrosis? *Eur Respir J*, 2017;50:1701360
14. Oda T, Sekimoto T, Kurashima K, et al. Acute HSF1 depletion induces cellular senescence through the MDM2-p53-p21 pathway in human diploid fibroblasts. *J Cell Sci*, 2018;131:jcs210724
15. Eckner R. p53-dependent growth arrest and induction of p21: A critical role for PCAF-mediated histone acetylation. *Cell Cycle*, 2012;11:2591-92
16. Lomas NJ, Watts KL, Akram KM, et al. Idiopathic pulmonary fibrosis: Immunohistochemical analysis provides fresh insights into lung tissue remodelling with implications for novel prognostic markers. *Int J Clin Exp Pathol*, 2012;5:58-71
17. Reya T, Clevers H. Wnt signalling in stem cells and cancer. *Nature*, 2005;434:843-50
18. Lehmann M, Hu Q, Hu Y, et al. Chronic WNT/ $\beta$ -catenin signaling induces cellular senescence in lung epithelial cells. *Cell Signal*, 2020;70:109588
19. Dao K-HT, Rotelli MD, Petersen CL, et al. FANCL ubiquitinates  $\beta$ -catenin and enhances its nuclear function. *Blood*, 2012;120:323-34
20. Wang X, Zhu Y, Sun C, et al. Feedback activation of basic fibroblast growth factor signaling via the Wnt/ $\beta$ -catenin pathway in skin fibroblasts. *Front Pharmacol*, 2017;8:32
21. Kvell K, Fejes AV, Parnell SM, Pongracz JE. Active Wnt/ $\beta$ -catenin signaling is required for embryonic thymic epithelial development and functionality *ex vivo*. *Immunobiology*, 2014;219:644-52
22. Yang HL, Tsai YC, Korivi M, et al. Lucidone promotes the cutaneous wound healing process via activation of the PI(3)K/AKT, Wnt/ $\beta$ -catenin and NF- $\kappa$ B signaling pathways. *Biochim Biophys Acta Mol Cell Res*, 2017;1864:151-68
23. Donmez D, Simsek O, Izgu T, et al. Genetic transformation in citrus. *Sci World J*, 2013;2013:491207
24. Velasco R, Licciardello C. A genealogy of the citrus family. *Nat Biotechnol*, 2014;32:640-42
25. Guo J, Fang Y, Jiang F, et al. Neohesperidin inhibits TGF- $\beta$ 1/Smad3 signaling and alleviates bleomycin-induced pulmonary fibrosis in mice. *Eur J Pharmacol*, 2019;864:172712
26. Gao Z, Wang ZY, Guo Y, et al. Enrichment of polymethoxyflavones from Citrus reticulata "Chachi" peels and their hypolipidemic effect. *J Chromatogr B Analyt Technol Biomed Life Sci*, 2019;1124:226-32
27. Castro MA, Rodenak-Kladniew B, Massone A, et al. Citrus reticulata peel oil inhibits non-small cell lung cancer cell proliferation in culture and implanted in nude mice. *Food Funct*, 2018;9:2290-99
28. Xu JJ, Liu Z, Tang W, et al. Tangeretin from Citrus reticulata inhibits respiratory syncytial virus replication and associated inflammation *in vivo*. *J Agric Food Chem*, 2015;63:9520-27
29. de Moraes Barros HR, de Castro Ferreira TAP, Genovese MI. Antioxidant capacity and mineral content of pulp and peel from commercial cultivars of citrus from Brazil. *Food Chem*, 2012;134:1892-98
30. Gao X, Wang C, Ning C, et al. Hepatoprotection of auraptene from peels of citrus fruits against thioacetamide-induced hepatic fibrosis in mice by activating farnesoid X receptor. *Food Funct*, 2018;9:2684-94
31. Zhou XM, Huang MM, He CC, Li JX. Inhibitory effects of citrus extracts on the experimental pulmonary fibrosis. *J Ethnopharmacol*, 2009;126:143-48
32. Feng F, Wang Z, Li R, et al. Citrus alkaline extracts prevent fibroblast senescence to ameliorate pulmonary fibrosis via activation of COX-2. *Biomed Pharmacother*, 2019;112:108669
33. Miao J, Liu J, Niu J, et al. Wnt/ $\beta$ -catenin/RAS signaling mediates age-related renal fibrosis and is associated with mitochondrial dysfunction. *Aging Cell*, 2019;18:e13004
34. Gu Z, Tan W, Feng G, et al. Wnt/ $\beta$ -catenin signaling mediates the senescence of bone marrow-mesenchymal stem cells from systemic lupus erythematosus patients through the p53/p21 pathway. *Mol Cell Biochem*, 2014;387:27-37
35. Chen YT, Tsai MJ, Hsieh N, et al. The superiority of conditioned medium derived from rapidly expanded mesenchymal stem cells for neural repair. *Stem Cell Res Ther*, 2019;10:390
36. Ghosh AK, Rai R, Park KE, et al. A small molecule inhibitor of PAI-1 protects against doxorubicin-induced cellular senescence. *Oncotarget*, 2016;7:72443-57
37. Jadeja RN, Powell FL, Jones MA, et al. Loss of NAMPT in aging retinal pigment epithelium reduces NAD(+) availability and promotes cellular senescence. *Aging (Albany NY)*, 2018;10:1306-23
38. Heldin CH. Autocrine PDGF stimulation in malignancies. *Ups J Med Sci*, 2012;117:83-91
39. Demaria M, Ohtani N, Youssef SA, et al. An essential role for senescent cells in optimal wound healing through secretion of PDGF-AA. *Dev Cell*, 2014;31:722-33
40. Zank DC, Bueno M, Mora AL, Rojas M. Idiopathic pulmonary fibrosis: Aging, mitochondrial dysfunction, and cellular bioenergetics. *Front Med (Lausanne)*, 2018;5:10
41. Rother K, John C, Spiesbach K, et al. Identification of Tcf-4 as a transcriptional target of p53 signalling. *Oncogene*, 2004;23:3376-84
42. Niehrs C. Function and biological roles of the Dickkopf family of Wnt modulators. *Oncogene*, 2006;25:7469-81
43. Komarov PG, Komarova EA, Kondratov RV, et al. A chemical inhibitor of p53 that protects mice from the side effects of cancer therapy. *Science*, 1999;285:1733-37
44. Acosta JC, Banito A, Wuestefeld T, et al. A complex secretory program orchestrated by the inflammasome controls paracrine senescence. *Nat Cell Biol*, 2013;15:978-90
45. Wu Q, Zhou Y, Feng FC, et al. Probing into the mechanism of alkaline citrus extract promoted apoptosis in pulmonary fibroblasts of bleomycin-induced pulmonary fibrosis mice. *Evid Based Complement Alternat Med*, 2018;2018:9658950
46. Faner R, Rojas M, Macnee W, Agustí A. Abnormal lung aging in chronic obstructive pulmonary disease and idiopathic pulmonary fibrosis. *Am J Respir Crit Care Med*, 2012;186:306-13
47. Barnes PJ, Baker J, Donnelly LE. Cellular senescence as a mechanism and target in chronic lung diseases. *Am J Respir Crit Care Med*, 2019;200:556-64
48. Brandenberger C, Mühlfeld C. Mechanisms of lung aging. *Cell Tissue Res*, 2017;367:469-80
49. Chilosi M, Carloni A, Rossi A, Poletti V. Premature lung aging and cellular senescence in the pathogenesis of idiopathic pulmonary fibrosis and COPD/emphysema. *Transl Res*, 2013;162:156-73
50. Clevers H. Wnt/ $\beta$ -catenin signaling in development and disease. *Cell*, 2006;127:469-80
51. Nabhan AN, Brownfield DG, Harbury PB, et al. Single-cell Wnt signaling niches maintain stemness of alveolar type 2 cells. *Science*, 2018;359:1118-23



52. Chilosi M, Poletti V, Zamò A, et al. Aberrant Wnt/beta-catenin pathway activation in idiopathic pulmonary fibrosis. *Am J Pathol*, 2003;162:1495-502
53. Morita H, Komuro I. Heart failure as an aging-related phenotype. *Int Heart J*, 2018;59:6-13
54. Prieto JD, Álvarez M, Hierro MI, et al. Beta-catenin and p53 expression in topographic compartments of colorectal cancer and its prognostic value following surgery. *Ann Diagn Pathol*, 2017;31:1-8
55. Chen HQ, Zhao J, Li Y, et al. Epigenetic inactivation of LHX6 mediated microcystin-LR induced hepatocarcinogenesis via the Wnt/ $\beta$ -catenin and P53 signaling pathways. *Environ Pollut*, 2019;252:216-26
56. Damalas A, Kahan S, Shtutman M, Ben-Ze'ev A, Oren M. Deregulated beta-catenin induces a p53- and ARF-dependent growth arrest and cooperates with Ras in transformation. *EMBO J*, 2001;20:4912-22
57. Uhl FE, Vierkotten S, Wagner DE, et al. Preclinical validation and imaging of Wnt-induced repair in human 3D lung tissue cultures. *Eur Respir J*, 2015;46:1150-66
58. Wang J, Shou J, Chen X. Dickkopf-1, an inhibitor of the Wnt signaling pathway, is induced by p53. *Oncogene*, 2000;19:1843-48
59. Huelsken J, Behrens J. The Wnt signalling pathway. *J Cell Sci*, 2002;115:3977-78
60. Gu Z, Tan W, Feng G, et al. Wnt/ $\beta$ -catenin signaling mediates the senescence of bone marrow-mesenchymal stem cells from systemic lupus erythematosus patients through the p53/p21 pathway. *Mol Cell Biochem*, 2014;387:27-37